Electric field enhanced hydrogen storage on polarizable materials substrates

J. Zhou[a,b], Q. Wang[c], Q. Sun[a,c,1], P. Jena[c], and X. S. Chen[b]

[a]Department of Advanced Materials and Nanotechnology, and Center for Applied Physics and Technology, Peking University, Beijing 100871, China; [b]National Laboratory for Infrared Physics, Shanghai Institute of Technical Physics, Chinese Academy of Science, Shanghai 200083, China; and [c]Department of Physics, Virginia Commonwealth University, Richmond, VA 23284

Edited by Mildred Dresselhaus, Massachusetts Institute of Technology, Cambridge, MA, and approved January 6, 2010 (received for review May 22, 2009)

Using density functional theory, we show that an applied electric field can substantially improve the hydrogen storage properties of polarizable substrates. This new concept is demonstrated by adsorbing a layer of hydrogen molecules on a number of nanomaterials. When one layer of H_2 molecules is adsorbed on a BN sheet, the binding energy per H_2 molecule increases from 0.03 eV/H_2 in the field-free case to 0.14 eV/H_2 in the presence of an electric field of 0.045 a.u. The corresponding gravimetric density of 7.5 wt% is consistent with the 6 wt% system target set by Department of Energy for 2010. The strength of the electric field can be reduced if the substrate is more polarizable. For example, a hydrogen adsorption energy of 0.14 eV/H_2 can be achieved by applying an electric field of 0.03 a.u. on an AlN substrate, 0.006 a.u. on a silsesquioxane molecule, and 0.007 a.u. on a silsesquioxane sheet. Thus, application of an electric field to a polarizable substrate provides a novel way to store hydrogen; once the applied electric field is removed, the stored H_2 molecules can be easily released, thus making storage reversible with fast kinetics. In addition, we show that materials with rich low-coordinated nonmetal anions are highly polarizable and can serve as a guide in the design of new hydrogen storage materials.

energetics | kinetics | nanomaterials | polarization | reversibility

Hydrogen, the simplest and most abundant element in the universe, is an energy carrier which is expected to play a critical role in a decentralized energy infrastructure with many important advantages over other fuels. Unlike fossil fuels such as oil, natural gas, and coal that contain carbon, pollute the environment, contribute to global warming, and have limited supply, hydrogen is clean, environmentally friendly, nontoxic, and abundant. In addition, it is renewable and packs more energy per unit mass than any other fuel. However, its commercial use as an alternate energy source has substantial difficulties to overcome. Among these, the most difficult challenge is to find materials that can store hydrogen with large gravimetric and volumetric density and operate under ambient thermodynamic conditions. The Department of Energy (DOE) has set a target for the ideal hydrogen storage material system to have a gravimetric density of hydrogen of 6 wt% by 2010. Furthermore, the storage materials should be able to reversibly adsorb/desorb H_2 in the temperature range of −20 to 50 °C under moderate pressures (maximum 100 atm). The first requirement limits the choice of storage materials to elements lighter than Al, whereas the latter requires hydrogen binding to be between physisorption and chemisorption energies. Recently Bhatia and Myers (1) studied the optimum thermodynamic conditions for hydrogen adsorption employing the Langmuir equation and then derived relationships between the operating pressure of a storage tank and the enthalpy of adsorption required for storage near room temperature. They have found that the average optimal adsorption enthalpy should be 15.1 kJ/mol, if operated between 1.5 and 30 bar at 298 K. When the pressure is increased to 100 bar, the optimal value becomes 13.6 kJ/mol. Therefore the optimal adsorption energy for H_2 should be in the range of $0.1 \sim 0.2$ eV/H_2. Unfortunately, the above two requirements are difficult to satisfy simultaneously. The bonding of hydrogen in light elements is either too strong, as in light metal hydrides and organic molecules, or too weak, as in graphite and carbon and BN fullerenes and nanotubes (2–5). For example, although BH_3, NH_3, and $B_{12}H_{12}$ contain a high weight percentage of hydrogen, the kinetics of hydrogen release is poor because of the strong bonding of H with N or B.

To overcome the above problems and to balance both energetics and weight percentage, recent efforts have been devoted to design new materials with exposed metal sites following the mechanisms proposed by Kubas (6) and Niu et al. (7). The Kubas mechanism takes advantage of the unfilled *d* orbitals of transition-metal atoms where H_2 molecules donate electrons to the unfilled *d* orbitals and the transition metals back donate the electrons to the H_2 molecules. As a result, H_2 retains its molecular bond, but in a slightly stretched form. The work of Niu et al. (7) focused on metal cations where stretching of the molecular bond of H_2 is caused by charge polarization. The difficulty with the former approach is that transition-metal atoms tend to cluster (8–11), whereas in the latter the binding energy tends to be lower than the desired value, especially when hydrogen coverage increases (12, 13). Recent attempts have concentrated on using metal ions that carry multiple charges such as Mg^{2+} and Al^{3+} in light porous materials (14–16). Three different strategies have been employed to introduce exposed metal sites (14): (*I*) remove the metal-bound volatile species which typically function as terminal ligands, (*ii*) incorporate metal species, and (*iii*) impregnate materials with excess metal cations. However, experimentally these techniques are complicated and difficult to control because any available atoms or molecules in the environment saturate the exposed metal sites, thus diminishing expected hydrogen adsorption capacity.

In this study, we propose a different approach that would make materials synthesis less complicated while improving the thermodynamics and reversibility of hydrogen storage. Note that the mechanism that allows exposed metal cations to store hydrogen in quasi-molecular form is the polarization of the H_2 molecule caused by the electric field associated with point ions (7, 11). Can the same objective be achieved by directly applying an external electric field to hydrogen storage materials? We show that this is indeed possible by considering a single BN sheet, an AlN sheet, a silsesquioxane molecule, and a silsesquioxane sheet. Using first-principles calculations we find that in an applied electric field the electrons of the hydrogen molecules are polarized. The electrostatic interactions between the hydrogen molecules and the substrates greatly improve the storage performance. For example, when one layer of H_2 is adsorbed on the BN sheet with an electric field of 0.045 a.u., the binding energy is 0.14 eV/H_2, five times larger than the binding energy of 0.03 eV/H_2 in the

Author contributions: Q.S. designed research; J.Z., Q.W., and X.C. performed research; Q.S. and P.J. wrote the paper.

The authors declare no conflict of interest.

This article is a PNAS Direct Submission.

[1]To whom correspondence should be addressed. E-mail: sunqiang@pku.edu.cn.

absence of the electric field. The corresponding gravimetric density of hydrogen is 7.5 wt%. Once the applied electric field is removed, the system goes back to its original state and hydrogen molecules easily desorb, yielding good reversibility and fast kinetics.

We chose to begin our study with BN sheets. Since the discovery that graphene, a single sheet of graphite, can be experimentally isolated (17), considerable attention has been focused on synthesizing similar BN-based materials because *h*-BN manifests a structural variety similar to that of *h*-C and possesses the same crystal structure with very similar cell parameters. However, the electronic properties of BN are distinctly different. For example, *h*-C can be metallic, semiconducting, or semimetallic depending upon its dimensionality, size, and coordination, whereas *h*-BN is typically a wide-band gap semiconductor. Very recently, Han et al. (18) successfully synthesized a *mono-atomic-layered* BN sheet by using a chemical-solution-derived method starting from single-crystalline hexagonal boron nitride. Currently the single-layered BN sheet has become a new nanoplatform for manipulating the electronic structures and magnetism for various applications (19–22).

Results and Discussion

We first consider the interaction between a single H_2 molecule and a BN sheet. The relative stability of different configurations of the H_2 molecule on a BN sheet in an external electric field (selected as 0.040 a.u.) vertical to the sheet has been studied (Fig. 1). We considered four adsorption sites for the H_2 molecule on the BN sheet: directly on top of a B or N atom (on-top site), above the midpoint of a bond linking the B and N atoms (bridge site), and above the center of a honeycomb-like hexagon (hollow site). For each site, various initial orientations of the H_2 molecule have been studied. After optimization, we found that the H_2 molecule prefers to align along the *z* direction, parallel to the electric field. The lowest energy is found when the H_2 molecule adsorbs on the N atom.

With the help of Mulliken population analysis, we determined that the upper H atom is negatively charged, whereas the charge on the lower one is positive. This can be understood by the polarization effects of the electric field, because it "pushes" positive charges along its direction. Due to its large electronegativity, N attracts electrons from B. Thus, on the BN sheet, the N sites are electron rich and are easily polarized in the applied electric field in a way similar to the H_2 molecule. The electrostatic interaction between the H_2 and N makes N the favored site for H_2 absorption (Fig. 1*C*)

We have further studied the effect of electric field strength on hydrogen adsorption by focusing on the "on-top-site" N. The H–H bond length (R_1), distance between N atom and H_2 molecule (R_2), the dipole moment of H_2 molecule, and binding energy per H_2 are plotted as a function of the magnitude of the electric field in Fig. 2. The data are fitted with the curves. We see that the H–H bond length increases exponentially with increasing electric field strength. This is due to the polarization interaction induced by the electric field and concurrent binding with the BN sheet. Simultaneously, the distance between the H_2 molecule and the substrate decreases linearly as the electric field increases. This indicates that the interactions between the H_2 molecule and BN sheet can be easily tuned by the electric field. When the electric field reaches 0.050 a.u., the H–H bond length R_1 becomes 0.815 Å and the distance to the substrate is 2.255 Å, resulting in adsorption energy of 0.48 eV. When the electric field reaches 0.060 a.u., the H_2 molecule is dissociated and atomically bonded to the BN sheet, indicating that molecular hydrogen adsorption can be achieved only below a certain critical electric field. Furthermore, from Fig. 2*C* we find that the induced dipole moment of the H_2 molecule changes linearly with electric field. Thus, in a weak electric field, contributions from higher-order nonlinear terms can be neglected.

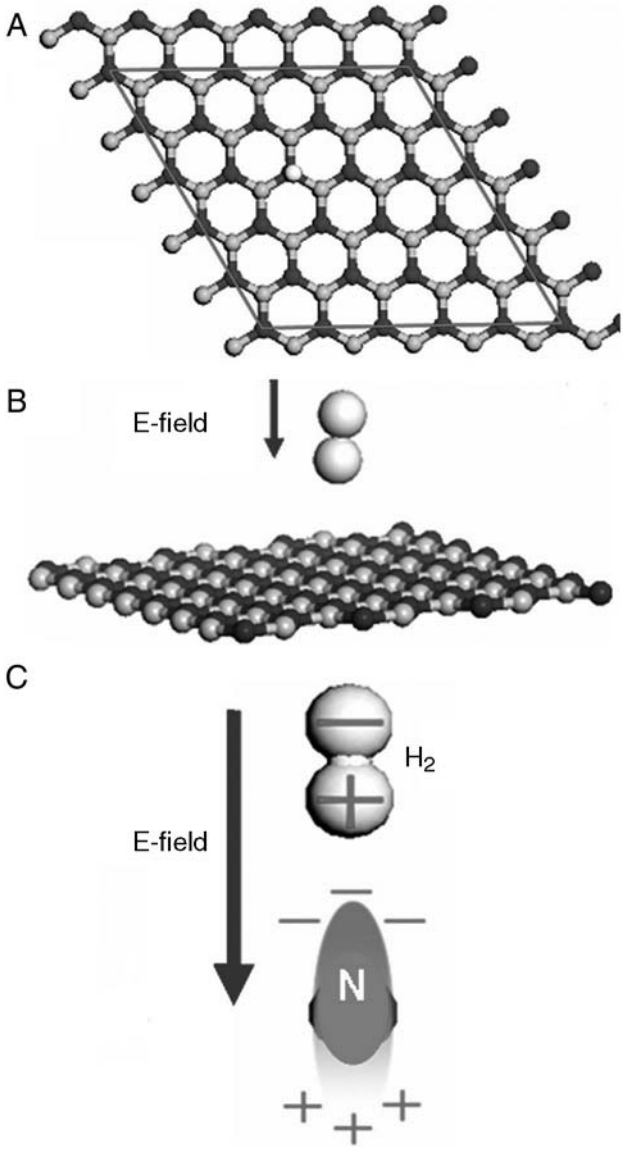

Fig. 1. Single H_2 molecule adsorbed on the BN sheet: (*A*) Top view; lines show the supercell used in simulations. (*B*) Side view; vertical electric field is applied in the –*z* direction. (*C*) Model demonstrating the polarized H_2 molecule and the polarized electrons at N site on the BN sheet.

We also quantitatively analyzed the adsorption energy, defined as, $E_b = E(\mathrm{BN}) + E(\mathrm{H_2}) - E(\mathrm{BN} + \mathrm{H_2})$. We found that the adsorption energy (E_b) changes with the applied field (E) in the following way (Fig. 2*D*):

$$1/E_b = 12.7684 - 10319.39^{*}E^2 + 4.19^{*}10^{6*}E^4 - 7.179^{*}10^{8*}E^6$$

According to classical physics's dipole–dipole interaction, E_b should scale with the distance R as $E_b \sim 1/R^3$. Because of the complicated induced polarization, in our case the relationship scales as $E_b \sim 1/R^{5.5}$ (as shown in Fig. 3), suggesting that the interactions between the polarized H_2 molecules and the polarized substrate are very short-ranged as compared to the classical long-range dipole–dipole interactions.

To investigate the effect of the electric field on the electronic structure, we plot the partial density of states of the system with and without the electric field (Fig. 4). In the absence of the electric field (Fig. 4*A*), the semiconductor nature of the BN sheet can be clearly seen. The corresponding energy band gap of 3.52 eV is less than that of the gap in the bulk phase, namely 5.97 eV (23).

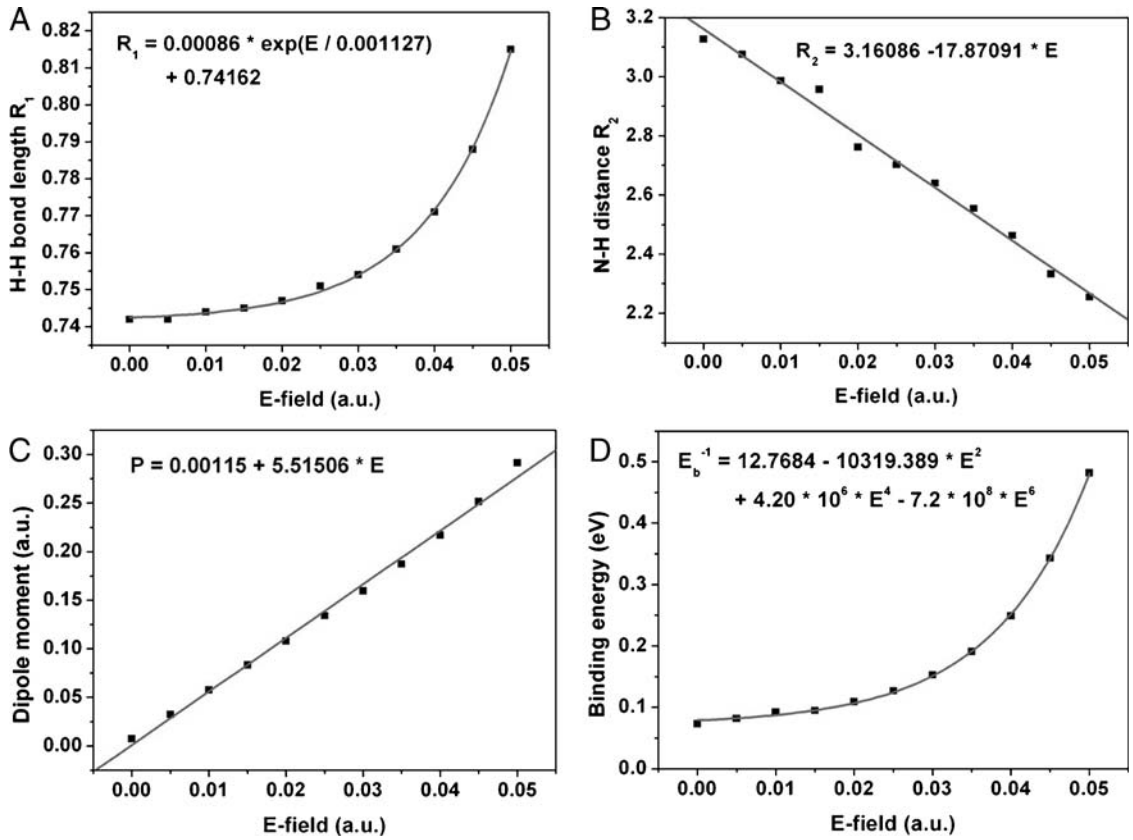

Fig. 2. Calculated data and fitted curve of (*A*) H–H bond length R_1 (in angstrom), (*B*) N-H distance R_2 (in angstrom), (*C*) induced dipole moment of H_2 molecule, and (*D*) binding energy as a function of electric field strength.

When the electric field of 0.05 a.u. is applied, the adsorption energy of the H_2 molecule is increased to 0.48 eV while the semiconductor property of the system is still retained (Fig. 4*B*), indicating that the BN sheet is not electrically broken down in an applied electric field. We also see that the peak in the *s* density of states at ~ -0.23 a.u. contributed by the H_2 orbital in the absence of the field shifts to a higher energy range (~ -0.12 a.u.) when the electric field is applied. Only the 2*p* orbitals of B and N atoms contribute to density of states at the Fermi level.

Next we study the case when one layer of H_2 molecule is adsorbed on the BN sheet (Fig. 5). We initially placed H_2 molecules with various orientations on four different adsorption sites as mentioned above. Once again, we found that the optimized H_2 molecules remain vertical to the sheet, i.e., parallel to the external electric field and the N on-top sites remain the favored adsorption sites. The changes in binding energy per H_2 molecule with different electric field are shown in Fig. 5*C*. We see that the binding energy increases from 0.03 eV/H_2 in the absence of the

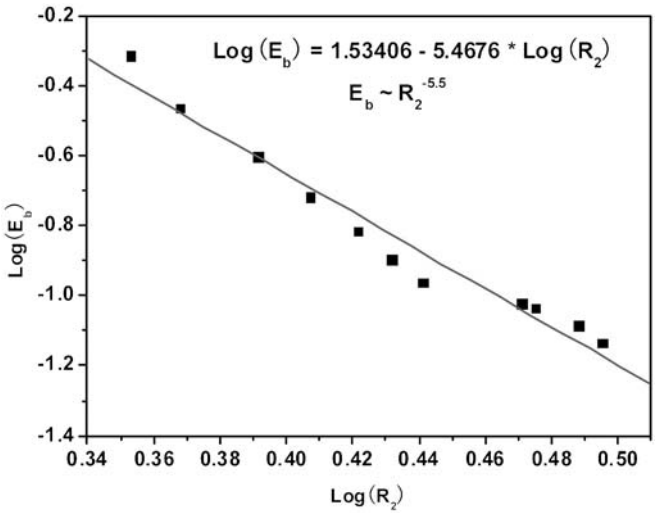

Fig. 3. Changes of adsorption energy E_b with distance R_2.

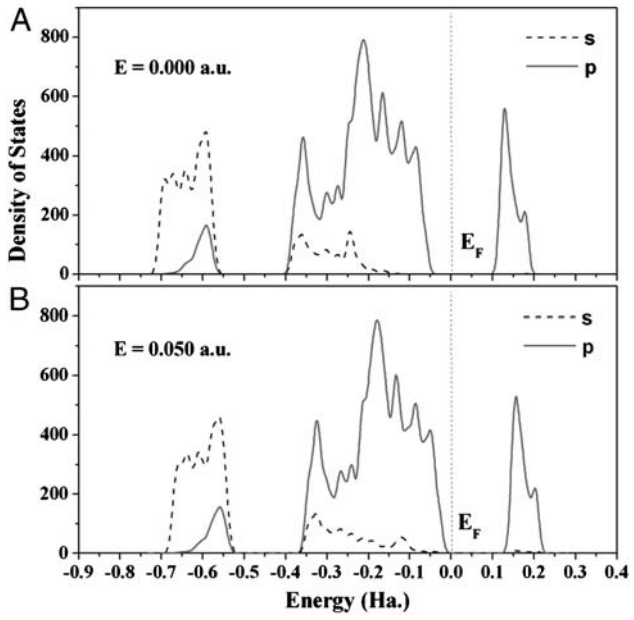

Fig. 4. Density of states of BN-H_2 with and without electric field. The vertical dashed line is for Fermi level.

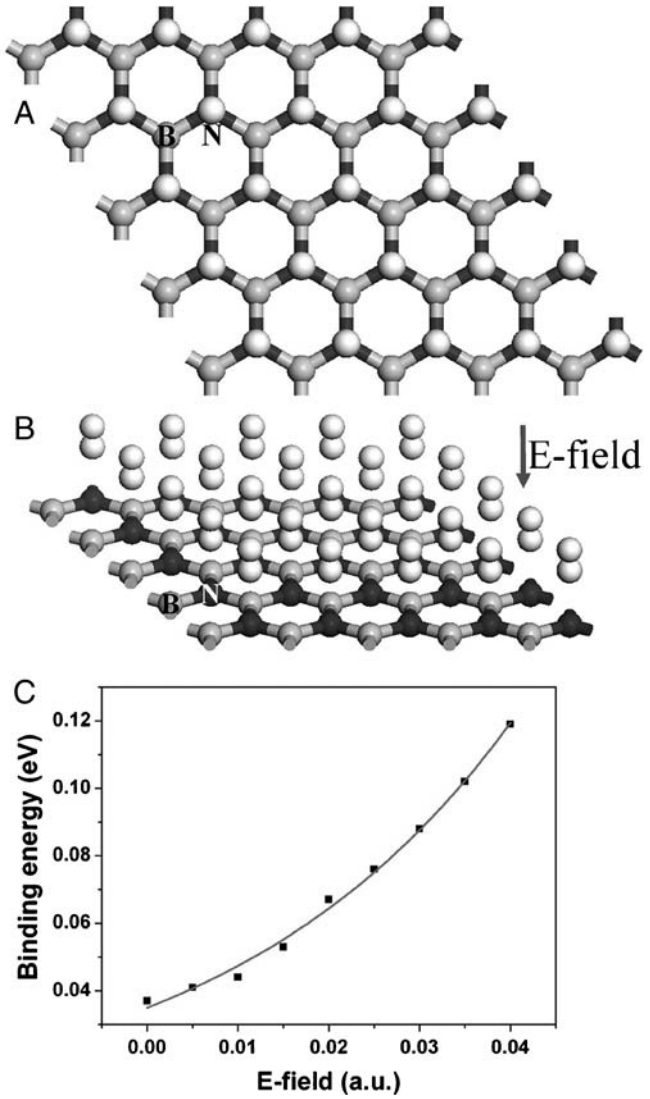

Fig. 5. Layer of H_2 molecules adsorbed on the BN sheet: (*A*) top view, (*B*) side view, (*C*) changes of binding energy with electric field.

electric field to 0.14 eV/H_2 in a field of 0.045 a.u. For a single H_2 molecule in the electric field of 0.045 a.u., the adsorption energy is much higher, 0.35 eV/H_2. There are two factors that account for this energy difference: (*i*) When one layer of H_2 molecules is introduced, their distance to the substrate increases due to steric hindrance. (*ii*) When a single H_2 molecule is absorbed on the BN sheet, because of the nonuniform adsorption, the substrate shows some geometric distortion near the adsorbing N site. However, the adsorption energy of 0.14 eV/H_2 is already within the energy window required for applications under ambient thermodynamic conditions (1). Equally important, the gravimetric density of stored hydrogen is 7.5 wt%. This is consistent with the 6 wt% system target set by DOE for 2010. To check the reversibility of hydrogen storage, we removed the external electric field and, as expected, found that all the adsorbed H_2 molecules become weakly bound with a binding energy of 0.03 eV/H_2. Therefore, storage and release of hydrogen can be easily achieved via switching on/off the external electric field.

To assess the feasibility that our study can lead to the focused discovery of unique hydrogen storage materials for practical applications, it is necessary to examine some of the assumptions we have made, the results we have obtained, and the conclusions we have drawn.

1. Because of the experimental success in synthesizing a single atomic BN layer (18), we chose a single BN sheet in our calculation to illustrate the mechanism. In fact, before the experimental synthesis, a single atomic BN layer was used as a theoretical model for hydrogen storage (20). However, it was found that the adsorption energy is only 0.04 eV/H_2, in agreement with our result of 0.03 eV/H_2 in the field-free case. Here we show that the applied external electric field can significantly enhance the hydrogen adsorption on a BN sheet. In practice, however, a single BN sheet is not enough for hydrogen storage and these sheets have to be assembled. Thus, one has to see if these sheets will collapse and adversely affect their hydrogen storage capacity. For this purpose, we have calculated the equilibrium distance (D) between two BN sheets stacked with five different stacking patterns and found that D lies in the range of $4.46 \sim 5.38$ Å. Because the equilibrium distance between the H_2 layer and the BN sheet is only 2.65 Å, the space between BN sheets for certain stacking configurations is enough to store H_2 molecules. One can also use some molecular linkers to assemble the sheets if larger separation is required.
2. We have used density functional theory with Becke-Lee-Yang-Parr (BLYP) exchange-correlation functional to calculate the adsorption energies of H_2 molecules. It is well known that density functional theory (DFT) does not treat van der Waals interactions accurately (24) and hence the accuracy of the calculated energetics of weakly bound systems can be called into question. Recently several authors (25, 26) have incorporated long-range dispersive interactions into DFT to treat weakly bound systems. They have found that the inclusion of long-range interaction increases the binding energies obtained using generalized gradient approximation (GGA) functionals in DFT. For example, Grimme (27) found that binding energy calculated using BLYP is about 2 kcal/mol (i.e., 0.087 eV) less than that calculated using quantum chemical method such as MP2. Therefore, our computed binding energy of 0.14 eV/H_2 is an underestimate and can increase to 0.23 eV/H_2 if more rigorous methods are used. This would bring our computed hydrogen adsorption energies even closer to the desirable energy window for applications.
3. Because DFT is not accurate in treating long-range interactions, one may wonder if it can accurately treat the interaction between the polarized H_2 molecules and substrate under the influence of an electric field. As mentioned above, DFT cannot treat long-range dispersive forces in van der Waals interaction properly. However, there is a difference between the range of dispersive force and the polarization force discussed here. In the former, the range has been experimentally identified to vary from 15 to 130 Å (28) where the electron densities nearly vanish. In the latter case, the distance between H_2 and the substrate is smaller than 3 Å, which is much less than the range of the dispersive force. Furthermore, the extended wave functions of 2p electrons in N sites and 1s electrons in H_2 result in a nonvanishing overlap of the electron densities between H_2 and the substrate. Consequently, the binding energy of hydrogen varies as $1/R^{5.5}$ where R is the distance between the H_2 molecule and the substrate. Note that the interaction energy due solely to dipole–dipole interaction varies as $1/R^3$. Therefore, we believe that the leading part of interaction between H_2 and the substrate can be calculated using DFT.
4. The electric field required to yield a binding energy of 0.14 eV/H_2 for H_2 adsorbed on a BN sheet is 0.045 a.u. This corresponds to an electric field of 23,000 MV/m which is very large. Therefore, the challenge now becomes how to reduce the required electric field. Based on the mechanism involved, we can expect that when a substrate is more polarizable than BN the required H_2 adsorption energy can be achieved with a lower electric field. To demonstrate this possibility, we repeated the calculations for H_2 adsorption on a single AlN

sheet, where Al replaces B in the BN sheet. Because more charges are transferred from Al sites to N sites in AlN compared to that in BN, it should be easier to polarize AlN. Indeed this is the case. In agreement with previous studies (29, 30), we found that without an electric field H_2 molecules are only weakly adsorbed on AlN nanostructures with small curvatures. When an electric field is applied to the AlN sheet, N sites become more favorable than Al sites for binding to hydrogen, and an electric field of 0.03 a.u. (15,000 MV/m) is needed to reach the same adsorption energy of 0.14 eV/H_2 as the BN sheet. To see if the applied electric field can be further reduced, we studied silsesquioxane ($H_8Si_8O_{12}$) (SQ). This is a cage molecule with O_h symmetry. It has been found that cyclopentadiene (Cp) units capped with transition-metal atoms can be grafted on SQ which can then be used for hydrogen storage (31), whereas a bare SQ cannot absorb any H_2 molecule due to weak interaction. The situation becomes totally different when an electric field is applied as the O sites become the absorption sites for H_2 molecules. We found that an electric field of 0.005 a.u. can result in absorption energy of 0.11 eV/H_2, as shown in Fig. 6. This electric field is an order of magnitude smaller than that in either the BN or AlN sheet. The main reasons are as follows: In an SQ cage, oxygen is 2-fold coordinated with Si, having approximately one electron transferred from Si to O. In addition, O-2*p* orbitals are predominant in the highest occupied molecular orbital (31). These factors make the O sites in an SQ cage highly polarizable. When SQ units are assembled on a nanosheet (Fig. 7), the absorption energy becomes 0.1 eV/H_2 for the same electric field of 0.005 a.u. (or 2571 MV/m). The above results suggest that anions with low coordination are highly polarizable in an electric field and hence can become the favorable sites for hydrogen adsorption. This can become an important principle in materials design for hydrogen storage, which is complementary to the existing principle that cations with low coordination (also called as exposed metal ions) have enhanced ability for hydrogen adsorption (7, 11, 14–16). Therefore, the synthesis of new anion rich materials with low coordination can further reduce the strength of the applied electric field.

5. From the preceding, we have seen that as the substrate gets more polarizable the required electric field strength becomes smaller. However, one has to affirm that the material can withstand the required field. There are two issues worthy of consideration: First, the magnitude of the external electric field necessary to breakdown materials depends on their dimensionality and structures. For example, the breakdown electric field for bulk SiO_2 is 1,500 MV/m, which increases to 2,200 MV/m in SiO_2 nanowire (32), and 1,800–2,700 MV/m in SiO_2 thin film (33). Second, the required external breakdown electric field is much less than the local electric field produced by metal ions. Here we take a Li^+ ion as an example to see how large an electric field it can produce. Note that the electric field (E) at a distance R from a Li^+ ion in free space is given by $E = e/[4\pi\varepsilon R^2]$, where $e = 1.602 \times 10^{-19}$ C (electronic charge), and $\varepsilon = 8.854 \times 10^{-12}$ $C^2\,J^{-1}\,m^{-1}$ (permittivity of free space). Because the equilibrium distance between H_2 and a Li^+ ion in Li^+H_2 cluster is about 2 Å (7), the electric field produced by a Li^+ ion is 36,000 MV/m. This is much larger than the required breakdown electric field of 23,000 MV/m for a BN sheet. When a Li atom is allowed to interact with C_{60} charge transfer happens, because of the large electron affinity of C_{60}, thus making Li positively charged. It has been found that Li carries a charge of 0.74*e*, and the equilibrium distance of H_2 molecules to Li ion varies in the range of 2.2–2.68 Å (34). Thus, the electric field produced by the supported Li ion on C_{60} lies in the range of 22,000–14,800 MV/m. These are comparable to the external electric field needed for a BN sheet and AlN sheet, but larger than that for an SQ molecule or SQ sheet. It is interesting to note that even in such strong local electric fields, no local breaking of geometry has been observed in LiC_{60}. This suggests that nanomaterials can withstand strong electric fields.

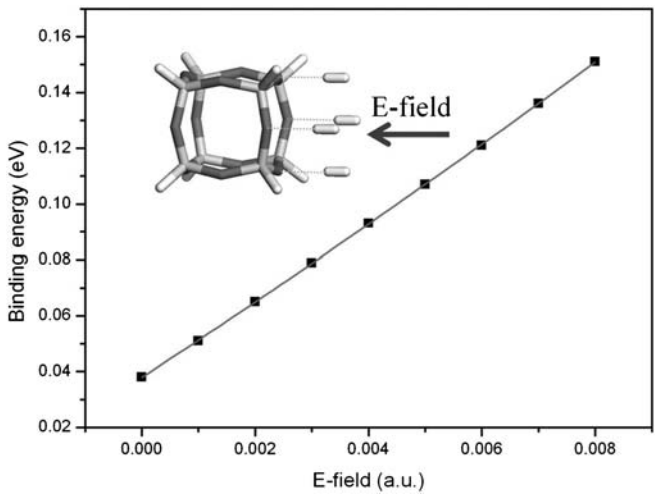

Fig. 6. Changes of binding energy of H_2 with SQ molecule in electric field.

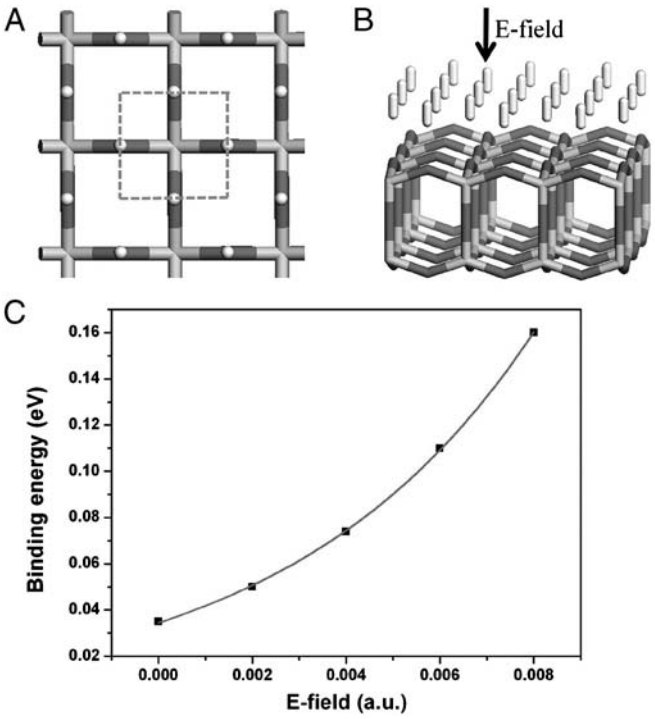

Fig. 7. Layer of H_2 molecules adsorbed on the SQ sheet: (*A*) top view, (*B*) side view, (*C*) changes of binding energy in electric field.

6. One may also wonder if a graphene sheet can be used to store hydrogen under the influence of an electric field. Indeed this was the first system we studied and found that the hydrogen adsorption energy was less than 0.10 eV/H_2 when the strength of the applied electric field was 0.045 a.u. This is consistent with the fact that a graphene sheet is less polarizable than a BN sheet. This result further proves that a highly polarizable substrate can serve as an effective hydrogen storage material for practical applications.

In conclusion, we have shown that application of an external electric field provides a unique pathway to store hydrogen and

PHYSICS

has the following advantages: (*i*) Contrary to the local electric field produced by exposed metal sites embedded in a substrate or a matrix, an external applied electric field is more effective and provides better control for reversible hydrogen storage. In particular, the energetics and kinetics can be manipulated by tuning the field strength. (*ii*) This process avoids complicated synthesis routes for embedding metal ions and does not suffer from the possibility that these ions may either cluster during repeated hydrogenation/dehydrogenation processes or be poisoned by other gases such as oxygen. (*iii*) In contrast to the ionic hydrides and alanates where the release of H_2 might render the materials unstable or incapable of reabsorption of H_2 if its chemical nature is altered, here the H_2 release can be very easily achieved by removing the electric field. (*iv*) The reversibility, kinetics, and material stability can be controlled by choosing appropriate electric field strength. (*v*) No catalysts are needed. (*vi*) The required external electric field can be smaller than the local electric field produced by metal ions.

Although many challenges still lie ahead in finding the right hydrogen storage material for practical applications, the aim of the present article is to demonstrate that an electric field can be used as an alternate parameter to tailor the thermodynamic and kinetic properties of storage materials. We not only provide a paradigm shift in our thinking of hydrogen storage but also provide a route to synthesize highly polarizable materials that are rich with *low-coordinated nonmetal anions*. We hope that this work will stimulate experimental research in this direction.

Methods

Our calculations are based on DFT with GGA for exchange and correlation potential for which BLYP (35) functional is used as implemented in DMol^3 package (36–38). The DMol^3 code has been extended to include not only the potential arising from the nuclear charges as "external" potential, but also the static potentials arising from an externally applied electric field. The Hamiltonian is composed of the potential arising from the external electric field (E_{ext}), kinetic operator T, and Hatree (V_H), and exchange-correlation (V_{xc}) potential.

$$H = T + V_H + V_{xc} - eE_{ext} \quad [1]$$

Using this prescription, Delley (39) studied the dissociation of molecules in strong electric fields and found that the bond length and vibrational frequency as a function of the field can be fit very well all the way up to the dissociation limit by an analytical formula derived from a Morse potential model, including an additional external electric field term.

All our calculations have been carried out using periodic boundary conditions on the *x* and *y* axes to simulate an infinite BN sheet. The electric field was applied in the *z* direction. The vacuum space of 15 Å is used in the direction normal to the BN sheet in order to avoid interactions between two layers. We have also repeated our calculations by using a larger vacuum space of 18 Å, but the results were found to be the same as those using 15 Å. Integrations over reciprocal space are based on Monkhorst-Pack scheme with $2 \times 2 \times 1$ and $9 \times 9 \times 1$ k-points grid meshes when either a single or a layer of H_2 is considered, respectively. We used a semicore pseudopotential with double-numerical basis set plus d functions. The orbital cutoff was set to be global and with a value of 3.4 Å. The atoms were relaxed without any symmetry constraints. Convergence in energy, force, and displacement was set at 2^*10^{-5} Ha, 0.001 Ha/ Å, and 0.005 Å, respectively. The accuracy of our exchange-correlation functional and basis set was tested through the following data. The bond length, binding energy, and polarizability of the H_2 molecule parallel to its axis are calculated to be 0.741 Å, 4.42 eV, and 6.0 a.u, respectively, which agree well with corresponding experimental values of 0.741 Å, 4.45 eV, and 6.3 a.u. The in-plane lattice parameter of the BN sheet has been optimized and the calculated value of 2.5 Å is also in good agreement with the experimental value of 2.505 Å.

ACKNOWLEDGMENTS. The authors are thankful to Mary Willis for a critical reading of the manuscript. This work is partially supported by grants from the National Natural Science Foundation of China (10874007, 20973010, 10725418, 10990100), the Foundation of National Laboratory for Infrared Physics, the National Grand Fundamental Research 973 Program of China (2010CB631301), the US National Science Foundation, and the US Department of Energy.

1. Bhatia SK, Myers AL (2006) Optimum Conditions for Adsorptive Storage. *Langmuir* 22:1688–1700.
2. Shiraishi M, Takenobu T, Ata M (2003) Gas-solid interactions in the hydrogen/ single-walled carbon nanotube system. *Chem Phys Lett* 367:633–636.
3. Kajiura H, et al. (2003) Hydrogen storage capacity of commercially available carbon materials at room temperature. *Appl Phys Lett* 82:1105–1107.
4. Dodziuk H, Golgonos G (2002) Molecular modeling study of hydrogen storage in carbon nanotubes. *Chem Phys Lett* 356:79–83.
5. Sun Q, Wang Q, Jena P (2005) Storage of molecular hydrogen in B-N cage: Energetics and thermal stability. *Nano Lett* 5:1273–1277.
6. Kubas GJ (1988) Molecular hydrogen complexes: Coordination of a σ bond to transition metals. *Acc Chem Res* 21:120–128.
7. Niu J, Rao BK, Jena P (1992) Binding of hydrogen molecules by a transition-metal ion. *Phys Rev Lett* 68:2277–2280.
8. Sun Q, Wang Q, Jena P, Kawazoe Y (2005) Clustering of Ti on a C_{60} surface and its effect on hydrogen storage. *J Am Chem Soc* 127:14582–14583.
9. Zhao Y, Kim YH, Dillon AC, Heben MJ, Zhang SB (2005) Hydrogen storage in novel organometallic buckyballs. *Phys Rev Lett* 94:155504–155507.
10. Yildirim T, Ciraci S (2005) Titanium-decorated carbon nanotubes as a potential high-capacity hydrogen storage medium. *Phys Rev Lett* 94:175501–175504.
11. Yoon M, et al. (2008) Calcium as the superior coating metal in functionalization of carbon fullerenes for high-capacity hydrogen storage. *Phys Rev Lett* 100:206806–206809.
12. Sun Q, Jena P, Wang Q, Marquez M (2006) First-principles study of hydrogen storage on $Li_{12}C_{60}$. *J Am Chem Soc* 128:9741–9745.
13. Sun Q, Wang Q, Jena P (2009) Functionalized heterofullerenes for hydrogen storage. *Appl Phys Lett* 94:013111–013113.
14. Dinca M, Long JR (2008) Hydrogen storage in microporous metal-organic frameworks with exposed metal sites. *Angew Chem Int Edit* 47:6766–6779.
15. Lochan RC, Head-Gordon M (2006) Computational studies of molecular hydrogen binding affinities: The role of dispersion forces, electrostatics, and orbital interactions. *Phys Chem Chem Phys* 8:1357–1370.
16. Wang Q, Sun Q, Jena P, Kawazoe Y (2009) Mg-doped GaN nanostructures: Energetics, magnetism, and H_2 adsorption. *Appl Phys Lett* 94:013108–013110.
17. Novoselov KS, et al. (2004) Electric field effect in atomically thin carbon films. *Science* 306:666–669.
18. Han WQ, Wu L, Zhu Y, Watanabe K, Taniguchi T (2008) Structure of chemically derived mono- and few-atomic-layer boron nitride sheets. *Appl Phys Lett* 93:223103–223105.
19. Park CH, Louie SG (2008) Energy gaps and stark effect in boron nitride nanoribbons. *Nano Lett* 8:2200–2203.
20. Shevlin SA, Guo ZX (2007) Hydrogen sorption in defective hexagonal BN sheets and BN nanotubes. *Phys Rev B* 76:024104–024114.
21. Si MS, Xue DS (2007) Magnetic properties of vacancies in a graphitic boron nitride sheet by first-principles pseudopotential calculations. *Phys Rev B* 75:193409–193412.
22. Baowan D, Cox BJ, Hill JM (2008) Junctions between a boron nitride nanotube and a boron nitride sheet. *Nanotechnology* 19:075704–075715.
23. Watanabe K, Taniguch T, Kanda H (2004) Direct-bandgap properties and evidence for ultraviolet lasing of hexagonal boron nitride single crystal. *Nat Mater* 3:404–409.
24. Kohn W, Meir Y, Makarov DE (1998) van der Waals energies in density functional theory. *Phys Rev Lett* 80:4153–4156.
25. Sun YY, Kim YH, Lee K, Zhang SB (2008) Accurate and efficient calculation of van der Waals interactions within density functional theory by local atomic potential approach. *J Chem Phys* 129:154102–154108.
26. Thonhauser T, et al. (2007) Van der Waals density functional: Self-consistent potential and the nature of the van der Waals bond. *Phys Rev B* 76:125112–125122.
27. Grimme S (2004) Accurate description of van der Waals complexes by density functional theory including empirical corrections. *J Comput Chem* 25:1463–1472.
28. Israelachvili JN, Tabor D (1972) The measurement of van der Waals dispersion forces in the range 15 to 130 nm. *Proc R Soc Lond A* 331:19–38.
29. Wang Q, Sun Q, Jena P, Kawazoe Y (2009) Potential of AlN nanostructures as hydrogen storage materials. *ACS Nano* 3:621–626.
30. Zhou X, Wu M, Zhou J, Sun Q (2009) Hydrogen storage in Al-N cage based nanostructures. *Appl Phys Lett* 94:103105–103107.
31. Sun Q, Wang Q, Jena P, Reddy BV, Marquez M (2007) Hydrogen storage in organometallic structures grafted on silsesquioxanes. *Chem Mater* 19:3074–3078.
32. Sun Q, Wang Q, Kawazoe Y, Jena P (2004) Soft breakdown of an insulating nanowirein an electric field. *Nanotechnology* 15:260–263.
33. Jeffery S, Sofield CJ, Pethica JB (1998) The influence of mechanical stress on the dielectric breakdown field strength of thin SiO2 films. *Appl Phys Lett* 73:172–174.
34. Chandrakumar KRS, Ghosh SK (2008) Alkali-metal-induced enhancement of hydrogen adsorption in C_{60} fullerene: An ab initio study. *Nano Lett* 8:13–19.
35. Becke AD (1993) Density-functional thermochemistry III. The role of exact exchange. *J Chem Phys* 98:5648–5652.
36. Delley B (1990) An all-electron numerical method for solving the local density functional for polyatomic molecules. *J Chem Phys* 92:508–517.
37. Delley B (2000) From molecules to solids with the DMol^3 approach. *J Chem Phys* 113:7756–7764.
38. Delley B (2002) DMol^3. (Accelrys, San Diego, CA) Ver. 4.2.
39. Delley B (1998) Vibrations and dissociation of molecules in strong electric fields: N_2, NaCl, H_2O, and SF_6. *J Mol Struct—Theochem* 434:229–237.